



SEDIMENTOLOGICAL AND HEAVY MINERALS STUDIES ON STREAM SEDIMENTS, EL-SHEIKH ABDELAL TOMB - EL-FAWAKHIR, CENTRAL EASTERN DESERT, EGYPT

Elshahat, O. R.

Geology Department, Faculty of Science, Al-Azhar University, Cairo, Egypt, 11884

osamaramzy80@azhar.edu.eg

ABSTRACT

The wadi deposit samples collected along the Qift -El Quseir paved Road between El-Sheikh Abdelal tomb and El-Fawakhir gold mine are subjected to mineralogical and chemical analyses. The textural studies of the alluvial sediments clearly establish that these sediments are fine to very coarse-grained, poorly sorted, very fine-very coarse skewed, very platy to extremely leptokurtic deposited under moderate to low energy conditions.

The heavy magnetic minerals are chiefly magnetite and goethite pseudomorph after pyrite while the non-magnetic are the metallic mineral rutile, the non-metallic minerals are albite, apatite, sphene, cetrine, fluorite, sillimanite, tourmaline and garnet which, related to the metamorphic rocks exposed at Abu Fannani schist in Meatiq and Abu Zeran areas and mafic silicate minerals pyroxene, biotite, hornblende and epidote which, related to mafic-ultramafic rocks of El-Fawakhir ophiolite sequences. The light minerals are mainly quartz, muscovite and potash feldspars related to the alkali feldspar granites, syenogranites, monzogranite, granodiorites, tonalite, quartz diorite rocks and quartz plugs exposed at Abu Ziran, Um Selimate, Wadi Attala and Wadi El-Haramiya.

Keywords: Grain size, standard deviation, skewness, kurtosis, graphic mean, depositional environment, heavy minerals.

INTRODUCTION

The study area is located in the Central Eastern Desert of Egypt between lat. $25^{\circ} 58' 01''$ and $26^{\circ} 07' 26''$ N and long. $33^{\circ} 36' 58''$ and $33^{\circ} 55' 58''$ E extending for about 53 Km long of the Qift -El Quseir paved Road (from El-Sheikh Abdelal tomb to El-Fawakhir gold mine). The climate of the region is extremely arid, with rainfall averaging less than 1 cm. per year, and daytime temperatures averaging 20 to 30 °C. The studied area is dissected by the main wadies Elharamia, Um Qarate, Abu Zeran, Um Sghuer, Um Ash Elhamra and Abu Mroua (Fig. 1).

Fig. 1: Landsat image showing the distribution of the studied samples and the main wadies in the study area.



The Precambrian basement complex in the Central Eastern Desert of Egypt have been studied by El Ramly, 1972, Akaad and Noweir 1980 and Kröner et al., 1994. Sedimentation, ore deposits and lithochemical surveys for ore metals and industrial uses of the alluvial sediments in some localities in Central Eastern Desert were studied by Morsy, 2000, Hassaan et al., 2014 and Attia et al., 2015.

The present investigation aims at studying the alluvial sediments for understanding the textural characteristics and heavy mineral constituents in relation to the rocks exposed on both banks of the Qift-El Quseir road.

The exposed rock units of the basement rocks forming the two banks of the studied alluvial sediments taken from the EGASMA map of Al Qusayr quadrangle are dismember ophiolite sequence, metavolcanics and meta-volcano-sedimentary rocks (Fig. 2).

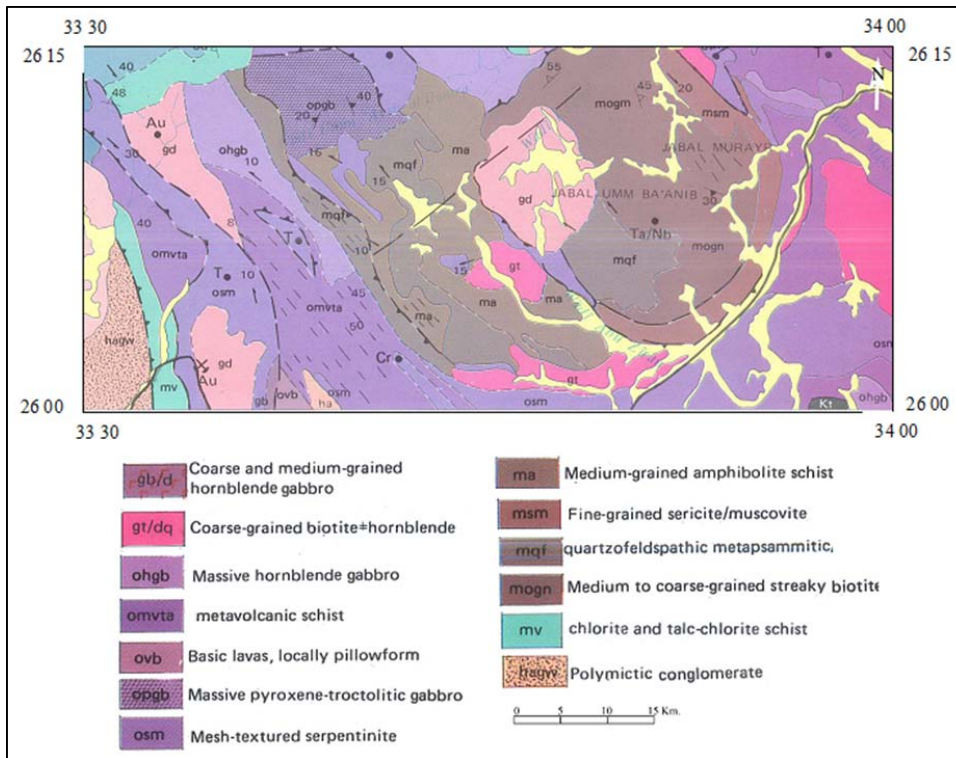


Fig. 2: Geological map of the study area (EGASMA 1992).

METHODOLOGES

A total of 28 alluvial samples were collected at depths of 20-50cm, these samples have been subjected to size analysis (Carver, 1971) and grain size parameters were calculated (Folk and Ward, 1957).

For the present study, GRADISTAT, v. 8.0 program developed by Blott and Pye (2001) was used, the different percentiles were obtained in phi units from the cumulative curves using the phi scale. The four sedimentological statistical parameters namely; The Graphic Mean (M_z), the Inclusive Graphic Standard Deviation (σ_i), the Inclusive Graphic Skewness (Sk_1) and the Graphic Kurtosis (K_G) were calculated for each sample, following Folk and Ward 1957.

All the collected samples were subjected for heavy mineral separation. Moreover, EDX chemical analyses were carried out for the separated heavy fraction of each treated sample using a Phillips XL-30 Environmental Scanning Electron Microscope (ESEM) in the laboratories of Nuclear Materials Authority.

RESULTS AND DISCUSSION**Grain size distribution**

The obtained grain size statistical parameters for the studied sediments are represented in tables 1 & 2.

A total of 24 samples exhibit have unimodal grain-size distribution patterns. The modal class falls within the coarse - very coarse sand. Only four samples show bimodal distribution (Table1), must probably related to site of these samples at plain of two or more than one tributaries (Fig. 1). The cumulative curves show almost similar trends exhibiting predominant sand size.

Table 1: The distribution of the statistical parameters of studied sediments.

S. No.	Mean Size (MZ)	Standard Deviation (σ_1)	Skewness (SKI)	Kurtosis (KG)	Remarks				Gravel %	Sand %	Mud %	Sample Type	Texture group
					CS	PSo	VFSk	VPK _g					
1	0.112	1.16	0.725	0.481	CS	PSo	VFSk	VPK _g	41	56.2	2.8	Un, PSo	SG
2	1.868	1.448	-0.178	1.298	MS	PSo	CSk	LK _g	10.3	85.7	4.1	Un, PSo	GS
3	-0.843	0.488	3.936	4.47	VCS	WSo	VFSk	ELK _g	74.1	25.2	0.7	Un, WSo	SG
4	1.227	1.963	-0.264	0.612	MS	PSo	CSk	VPK _g	19.7	75.3	5	Un, PSo	GS
5	1.053	1.611	-0.203	1.086	MS	PSo	CSk	MK _g	12	86.9	1.1	Un, PSo	GS
6	0.225	1.249	0.043	0.743	CS	PSo	SSk	PK _g	20.3	79.1	0.7	Un, PSo	GS
7	-0.176	1.45	0.31	0.53	VCS	PSo	VFSk	VPK _g	32.6	66.2	1.2	Un, PSo	SG
8	2.04	1.34	0.058	1.119	FS	PSo	SSk	LK _g	1.9	93	5.1	Un, PSo	SGS
9	0.237	1.521	0.64	0.452	CS	PSo	VFSk	VPK _g	39.9	57.4	2.7	Un, PSo	SG
10	-0.059	1.754	0.474	0.664	VCS	PSo	VFSk	VPK _g	33.8	63	3.1	Un, PSo	SG
11	-0.396	1.124	1.566	1.035	VCS	PSo	VFSk	MK _g	58	39	3	Un, PSo	SG
12	-0.342	1.083	1.706	0.761	VCS	PSo	VFSk	PK _g	56.50	41.30	2.20	Un, PSo	SG
13	0.122	1.521	1.416	0.683	CS	PSo	VFSk	PK _g	54.50	40.60	4.80	Bi, PSo	MSG
14	-0.535	0.963	2.057	1.02	VCS	MSo	VFSk	MK _g	60.80	36.80	2.30	Bi, MSo	SG
15	0.936	2.003	-0.015	0.591	CS	VPSo	SSk	VPK _g	22.50	71.80	5.70	Bi, VPSo	GS
16	-0.323	1.334	0.452	0.525	VCS	PSo	VFSk	VPK _g	36.10	62.50	1.30	Un, PSo	SG
17	0.666	1.596	-0.084	0.403	CS	PSo	SSk	VPK _g	29.50	86.60	2.00	Un, PSo	SG
18	-0.177	1.271	0.868	0.494	VCS	PSo	VFSk	VPK _g	44.90	53.30	1.80	Un, PSo	SG
19	0.468	1.735	0.054	0.61	CS	PSo	SSk	VPK _g	24.30	73.60	2.10	Un, PSo	GS
20	-0.682	0.649	1.862	0.573	VCS	MWSo	VFSk	VPK _g	58.70	40.80	0.40	Un, MWSo	SG
21	1.242	1.365	-0.19	1.303	MS	PSo	CSk	LK _g	12.90	85.10	2.00	Un, PSo	GS
22	-0.497	0.885	1.985	0.763	VCS	MSo	VFSk	PK _g	58.60	40.00	1.40	Bi, MSo	SG
23	-0.435	1.406	0.539	0.585	VCS	PSo	VFSk	VPK _g	38.30	60.40	1.20	Un, PSo	SG
24	0.513	1.554	0.076	0.86	CS	PSo	SSk	PK _g	19.40	78.40	2.30	Un, PSo	GS
25	-0.165	1.421	0.265	0.642	VCS	PSo	Fsk	VPK _g	30.70	67.90	1.40	Un, PSo	SG
26	-0.527	1.041	0.826	0.504	VCS	PSo	VFSk	VPK _g	46.10	52.60	1.30	Un, PSo	SG
27	-0.296	1.105	1.246	0.696	VCS	PSo	VFSk	PK _g	51.60	45.90	2.50	Un, PSo	SG
28	-0.36	1.44	0.403	0.812	VCS	PSo	VFSk	PK _g	33.10	65.40	1.40	Un, PSo	SG
MIN.	-0.06	0.48	-0.015	0.4					1.9	25.2	0.7		
MAX	2.04	2	3.93	4.47					74.1	86.9	5.7		
AVG	0.175	1.33	0.77	0.86					36.5	61.78	2.34		

CS: Coarse Sand, MS: Medium Sand, VCS: Very Coarse Sand, FS: Fine Sand, PSo: Poorly Sorted, VPSo: Very Poorly Sorted, WSo: Well Sorted, MSo: Moderately Sorted, MWSo: Moderately Well Sorted, VFSk: Very Fine Skewness, CSk: Coarse Skewness, S: Symmetrical, Fsk: Fine Skewness, VPK_g: Very Platykurtic, LK_g: Leptokurtic, ELK_g: Extremely Leptokurtic, M: Mesokurtic, PK_g: Platykurtic, Un: Unimodal, Bi: Bimodal, SG: Sandy Gravel, GS: Gravelly Sand, MSG: Muddy Sandy Gravel.

Table 2: Calculated percentages of the grain size parameters of the studied sediments.

Mean Size (M_z)			Standard Deviation (σ_1)			Skewness (Sk_1)			Kurtosis (K_G)		
Class	No. of Samples	%	Class	No. of Samples	%	Class	No. of Samples	%	Class	No. of Samples	%
VCS	15	53.57	PSo	23	82.14	VFSk	17	60.71	VPK _g	14	50
CS	8	28.57	VPSo	1	3.57	Fsk	1	3.57	PK _g	7	25
MS	4	14.28	MSo	2	7.14	S	6	21.42	M	3	10.71
FS	1	3.57	MWSo	1	3.57	CSk	4	14.28	LK _g	3	10.71
			WSo	1	3.57				ELK _g	1	3.57

Applying the textural classification adopted by Folk (1954), the sandy gravel (64 %) are the dominant and gravelly sand (28.5 %) while the slightly gravelly sand (3.5 %) and muddy sand gravel are minor sizes (3.5 %), (Table 1 and Fig. 3).

The graphic mean (M_z) of the samples chiefly within the very coarse (53.5 %) and the coarse (28.5 %), while the medium (14.2 %) and fine sand size (3.5 %) are minor sediment samples, (Tables 1 & 2 and Figs. 4 & 5).

The predominance of coarse - grained sediments and lack of fine sands suggests strong to moderate energy conditions of deposition (Singarasubramanian et al., 2006, Abdulkareem et al, 2011, Rajganapathi et al., 2013, Watson et al., 2013 and Amireh, 2014).

The sediments have variation of the inclusive graphic standard deviation (σ_i) (Fig. 6). They are chiefly poorly sorted (82.1 %), while very poorly sorted (3.5 %), moderately sorted (7.1 %), moderately well sorted and well sorted (3.5 % for each one), (Table 2). The poorly sorting of the studied sediments is due to short distance of transportation from the source rocks and the intermixing of sediments from different types of surrounding rock units (Venkatraman et al. 2011 and Muhs 2013), while the well sorted character of sediments indicates the winnowing or back and forth motion by the depositing agent.

The studied samples are chiefly very fine skewed (60.17%), while the symmetrical skewed (21.4 %), coarse skewed (14.2 %) and fine skewed (3.57%), (Table 2 and Figs 4 &7), indicates the prevalence of high and occasionally low energy wave of medium of transportation, entailing a mixed distribution of coarse and fine sediments (Rajasekhara et al., 2008).

Fig. 3: Plotting of the studied sediments on the ternary diagram proposed by Folk, 1954.

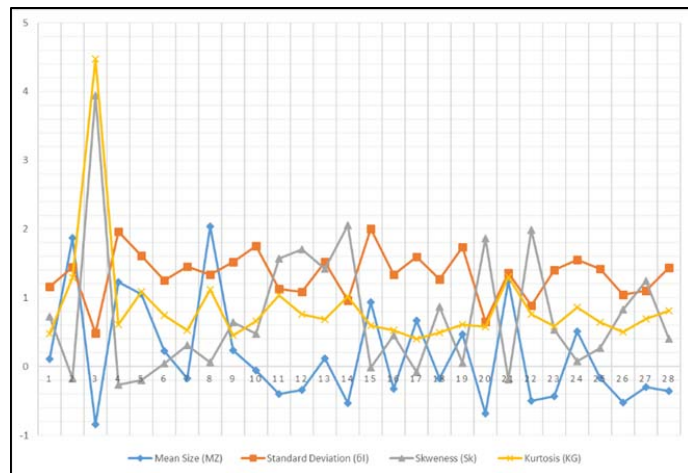
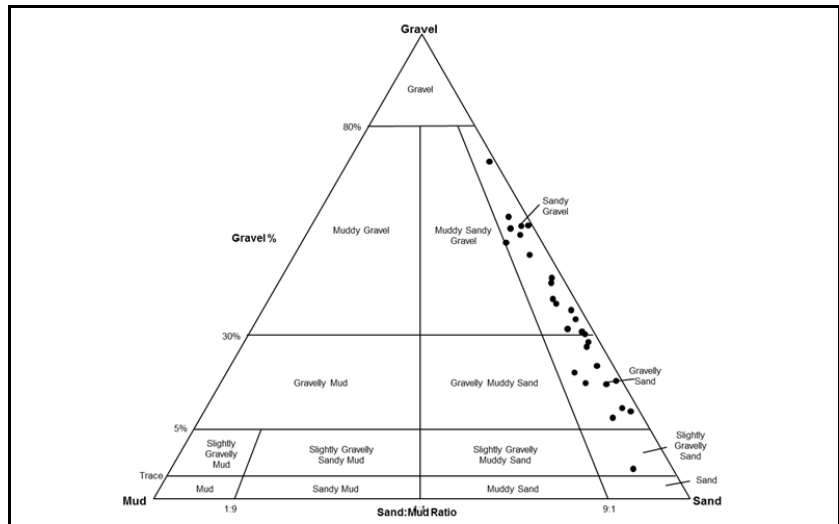


Fig. 4: Variation chart of the studied textural parameters for the studied samples.

Sedimentological and Heavy Minerals Studies On Stream Sediments

Fig. 5: Comparative histograms of main size for the studied samples.

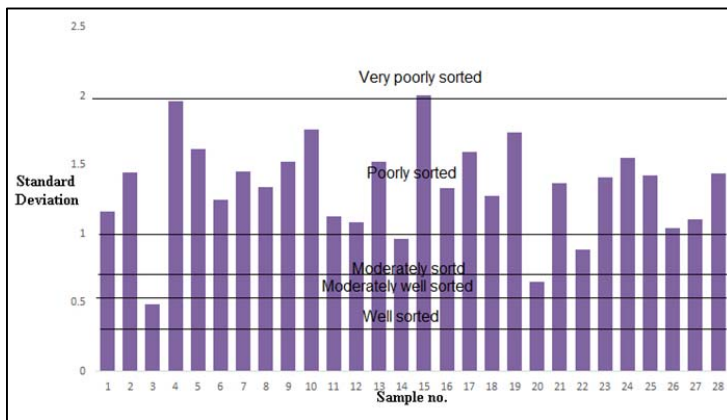
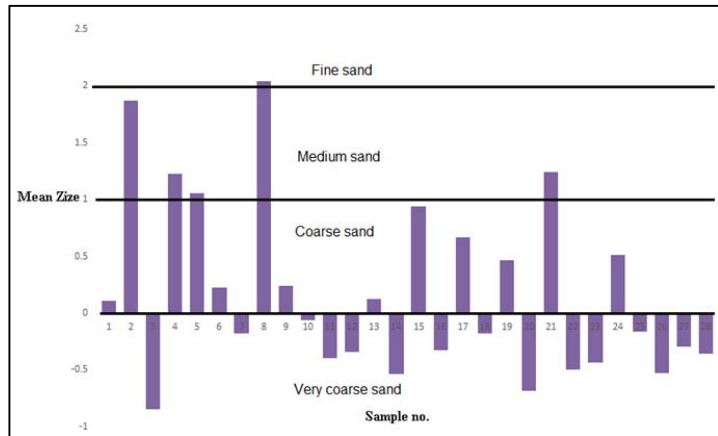
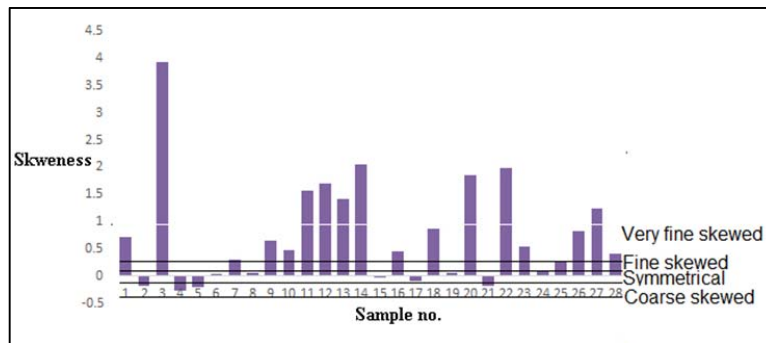


Fig. 6: Comparative histograms of sorting for the studied samples.

Fig. 7: Comparative histograms of skewness for the studied samples.



The studied samples are chiefly very platykurtic to platykurtic (75 %), while the mesokurtic to extremely leptokurtic are (24.9 %), (Table 2 and Figs 4 & 8). The studied sediments show wide range value of the kurtosis which suggests that sediment achieved its sorting elsewhere in high-energy environment (Baruah et al., 1997). The mesokurtic to leptokurtic samples refer to the continuous addition of finer or coarser sizes after the winnowing action and retention of their original characters during deposition (Avramidis et al. 2012). The samples possessing mesokurtic to platykurtic character indicate high energy, wide distribution and maturity of sediments (Venkatramanan et al., 2010 and Rajganapathi et al., 2013).

Results of the heavy mineral analysis

The results of the calculated heavy and light fractions for the samples, as well as amount (in wt %) of the mounted heavy minerals are given in tables (3 & 4) respectively. The light minerals are quartz, muscovite and potash feldspar, with an average of 88.5%, 6.92% and 4.52% respectively (Table 4). Quartz is generally represented by colorless angular to sub-angular and yet sub-rounded grains. Muscovite

minerals are transparent, colorless or tinted through grays of high birefringence for the irregular foliated and flaky forms. The potash feldspar minerals are varying from colorless to pale pink colored sub-angular to sub-rounded grains, recommend the presence of albite and potash feldspars respectively.

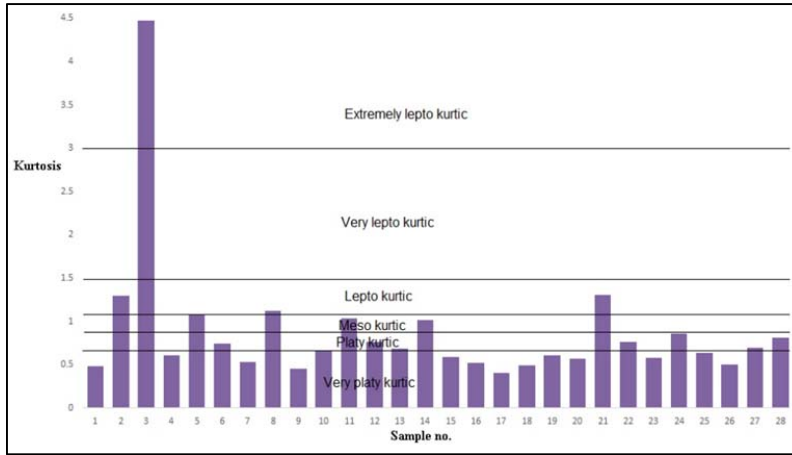


Fig. 8: Comparative histograms of kurtosis for the studied samples.

Table 3: Percentage of the investigated stream samples (%).

S. No.	Very fine sand size		Fine sand size	
	% of light minerals	% of heavy minerals	% of light minerals	% of heavy minerals
1	87.64	12.36	77.38	22.62
2	60.25	39.75	55.92	44.08
3	89.78	10.22	92.12	7.88
4	85.44	14.56	83.24	16.76
5	53.92	46.08	56.44	43.56
6	54.65	45.35	43.70	56.30
7	82.41	17.59	82.12	17.88
8	77.60	22.40	60.14	39.86
9	93.64	6.36	68.59	31.41
10	62.32	37.68	52.64	47.36
11	88.20	11.80	70.30	29.70
12	88.17	11.83	72.64	27.36
13	92.83	7.17	83.12	16.88
14	71.98	28.02	64.70	35.30
15	86.21	13.79	63.45	36.55
16	70.53	29.47	38.24	61.76
17	77.05	22.95	53.96	46.04
18	83.42	16.58	53.60	46.40
19	50.36	49.64	67.98	32.02
20	79.47	20.53	62.97	37.03
21	80.74	19.26	70.08	29.92
22	72.47	27.53	67.85	32.15
23	82.72	17.28	71.18	28.82
24	85.39	14.61	87.02	12.98
25	86.14	13.86	63.21	36.79
26	85.53	14.47	49.24	50.76
27	86.72	13.28	58.59	41.41
28	93.13	6.87	77.10	22.90

The recorded heavy mineral assemblages in the studied sediments are opaque (magnetite and goethite) and non-opaque (pyroxene, hornblende, biotite, albite, cetrine, sphene, sillimanite, garnet, apatite, fluorite, tourmaline, rutile, epidote and olivine) mineral groups. The heavy mineral assemblages were dominated by non-opaque minerals. The represented heavy minerals are hence subjected to chemical analyses using Scanning Electron Microscope (SEM). The results are given in Table (5) and figures 9 to 13.

Sedimentological and Heavy Minerals Studies On Stream Sediments

The heavy minerals constitute a relatively considerable amount of the samples varying from 6.36% to 49.64% and 7.88% to 61.76% of their content for the very fine and fine sand size respectively, (Table 3).

The opaque ore minerals titanomagnetite and goethite are the dominant. They form an amount varying from 5% to 41% (Table 4). Titanomagnetite displays metallic to dull luster composite grains with deep black color, their habit angular to sub-angular massive and granular grains (Fig. 9a). Titanomagnetite of homogenous and heterogeneous habit, usually associated with quartz, and potash feldspar as inclusions.

In El-Fawakhir mafic-ultramafic igneous rocks titanium is present mainly as titanomagnetite and ilmenite. This due to titanium replace silicon in crystalline silicates, because the titanium ion is too large to fit into a tetrahedral coordination of four oxygen ions. Also, titanium can replace Al in six coordination, it is probably captured by such minerals on account of its higher charge Ti^{4+} - Al^{3+} (Goldschmidt, 1954).

Table 4: Amount (wt %) of the mounted light and heavy minerals of the investigated samples.

	Light minerals															
	Qz	Pf	Mu													
Min.	64.2	1.2	0.5													
Max.	98	9.9	28.5													
Avg.	88.5	4.5	6.9													
	Heavy minerals															
	Py	Go	Ma	Bi	Pl	O	H	F	C	Ru	To	Ap	Ga	S	Si	Ep
Min.	17.5	3	2	3	0.5	0	4	0	0	0	0	0.5	0	0	0	0
Max.	70	20	21	12	10	6	14	3	1	0.8	1.2	6	0.6	0.5	0.8	0.8
Avg.	45.7	12.4	11.6	7.6	3.1	2.1	9.8	1.4	0.3	0.4	0.6	3.2	0.2	0.2	0.3	0.3

Qz: quartz, Pf: potash feldspar, Mu: muscovite, Py: pyroxene, Go: goethite, Ma: magnetite, Pl: plagioclase, Ba: barite, O: olivine, H: hornblende, F: fluorite, C: cetrine, Ru: rutile, To: tourmaline, AP: apatite, Ga: granite, S: sphene, Si: sillimanite, Ep: epidote.

Table 5: Chemical composition of some selected heavy minerals.

	Titano-Magnetite	Goethite	Enstatite	Augite	Hornblende	Biotite	Olivine	Apatite	Garnet	Albite	Tourmaline	Sphene
Fe	27.95	67.75	9.3-25.8	12.71	31.17	7.49	26.6	5.81	8.8-38.1	4.26	4.93	5.3-7
Si	2.21	21.77	35.5-50	32.24	30.96	34.08	36.2	3.07	29.3-33.5	59.67	46.32	13.7-18.3
Al	1.02	4.61	7.2-17.1	20.41	19.47	9.96	16.2	1.41	16.5-16.6	17.76	47.83	3-3.2
Ca		1.90	4-15.1	34.63	1.35	8.89		62.22	70.24	6.02		31.3-37.7
Ti	41.81		3.77			4.24			10.4-41	1.18		37.6-39
Mg		1.57	11.8-17		11.41	14.58	18.6	1.31		2.94	1.72	
Mn									5.32			
Cl												
K			1.7-1.8		2.22	0.76				2.27		
S												
O	27.01											
Na					1.66					5.97		
P								26.19				

Goethite is commonly angular to sub-rounded grains with submetallic or dull luster, no-cleavage of red, reddish black, yellowish and brownish yellow color (Fig. 9b). Goethite cubes are the alternation product of pseudo-morph after pyrite. At higher temperatures a very small amount of ferric iron seems to be able to enter 4-coordinated positions in silicates (Goldschmidt, 1954).

Monazite is detected in goethite grain with semi-quantitative chemical composition Ce 31.42%, La 30.41%, P 15.42% and Fe 10.14% with minor amount of Pr, Nd, Si, Al, U and K (Fig. 9b). Minor amount of aluminum and ferric iron may occur in the studied monazite. Monazite is moderately resistant to chemical weathering and is frequently concentrated as detrital minerals in El-Fawakhir stream sediments (Derr et al., 2001).

Pyroxene varieties range from black to dark and light green or white prismatic crystals to sub-angular grains with vitreous luster (Fig. 10). Both clinopyroxene: augite and orthopyroxene: enstatite detected. Mg and Fe^{2+} are regularly present in the orthopyroxenes. High Al content occurs mainly in orthopyroxenes of high grade metamorphic rocks at Meatiq and El-Fawakhir areas. From the microchemical analyses, the Al not greater than 20.41%. There is solid solution between enstatite and diopside and is not complete at solidus temperatures.

In many Mg- rich orthopyroxene of El-Fawakhir mafic and ultramafic rocks, the bulk of the Ca (Mg, Fe) Si₂O₆ initially in solid solution at the temperature of crystallization is exsolved on cooling.

Hornblende is often elongated and prismatic deep- green crystals (Fig. 11a). Hornblende Because hornblende form a complex solid solution series with several other amphibole minerals, localities for other species in the series will be cited (Derr et al., 2001). This due form pargasite (hornblende) in some El-Fawakhir gabbroic rocks.

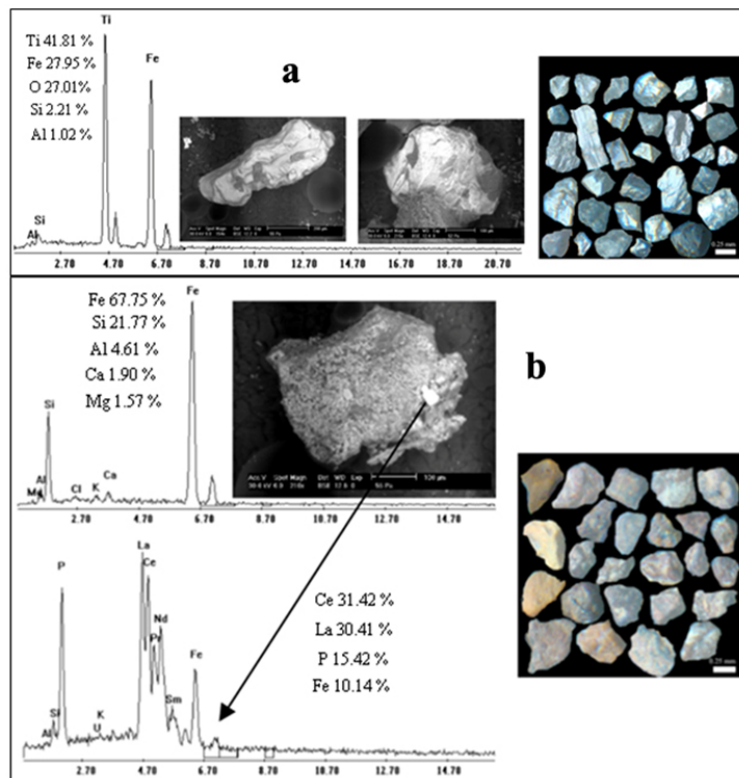
Biotite occurs as usual flakes of brown to yellowish brown, grey and some subhedral crystals are present (Fig. 11b). The composition of most biotites fall within the field outlined by four end-members, phlogopite, annite, eastonite and siderophyllite. Thus, in the studied biotite as compared with phlogopite, magnesium is replaced by ferrous iron and also trivalent ions (Fe⁺³, Al), and aluminum replaces silicon in tetrahedral sites (Deer et al., 2001). Also, there are other substitutions for K: Na and Ca occurred in the studied biotites. Calcium is usually present in higher concentration than the others in the present biotites.

Olivine occurs as sub-angular and sub-rounded grains with Pale olive green to yellow-green and transparent to translucent with a glassy luster (Fig. 11c). Based on the chemical composition the studied olivine is present as fayalite.

The recorded **apatite** is small prismatic well crystalline forms of good vitreous luster with indication of some inclusions inside the grains (Fig. 11d). In the studied apatite Ca may be partially replaced by Mg, Si and Fe. Various elements of Pb, Ba, Y, Sr and So₄ have been substituted in apatites (Goldschmidt, 1954 and Derr et al., 2001).

Garnet isn't an individual mineral but a group of minerals closely related in physical and chemical properties. Garnet is represented by dark brown to pale pink sub-rounded to rounded crystals with characteristic vitreous luster (Fig. 12a). In garnet molecules, each of the divalent metals Ca, Fe, Mg and Mn combining with each of the four trivalent metals Al, Fe, Mn and Cr. Some of the unusual combinations have been reported in the studied garnet hosted in Abu Fannani schists and Meatiq gneisses. The investigated garnet type is almandine-spessartine-grossular series, this due to substitute between iron, manganese and calcium.

Fig. 9: EDX semi-quantitative chemical analysis (Wt %), BSE and photomicrograph of a) titano-magnetite and b) goethite and monazite minerals.



Sedimentological and Heavy Minerals Studies On Stream Sediments

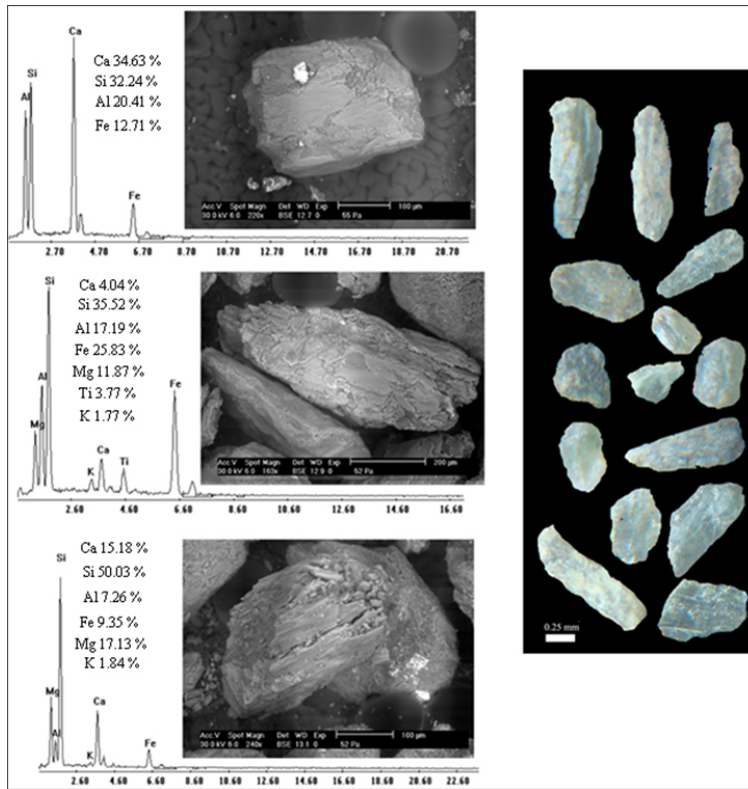
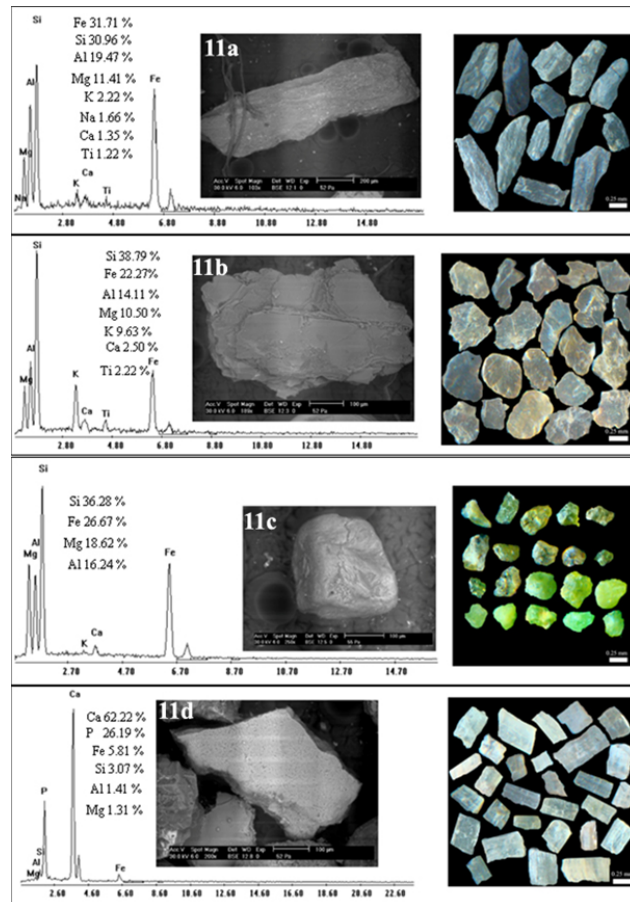


Fig. 10: EDX semi-quantitative chemical analysis (Wt %), BSE and photomicrograph of pyroxene minerals.

Fig. 11: EDX semi-quantitative chemical analysis (Wt %), BSE and photomicrograph of a) hornblende, b) biotite, c) olivine and d) apatite minerals.



Albite occur as white to gray yellowish, crystals with vitreous (glass-like) to porcelain-like luster (Fig. 12b).

Tourmaline represented by colorless, grey and greenish color, long slender to thick prismatic and columnar crystals with termination at one end (Fig. 12c). The chemistry of tourmaline is complex and until recently its basic formula was uncertain. In the formula $\text{Na R}_3\text{Al}_6\text{B}_3\text{Si}_6\text{O}_{27}(\text{OH})_4$. Na may be partially replaced by K or by Ca. In the studied tourmaline crystals R can be predominantly Fe^{+2} (4.97%) as in schorl and Mg (1.72%) as in dravite.

Sphene yellowish to brownish yellow and has regular wedge shape with vitreous luster (Fig. 13).

Sillimanite is represented by with yellowish to dark yellowish-brown irregular, angular grains (somewhat platy) grains.

Epidote occurs as sub-angular and sub-rounded grains with pale greenish-yellow to lemon-yellow color.

Rutile occurs as angular of elongated shape and slightly rounded brown-red grains.

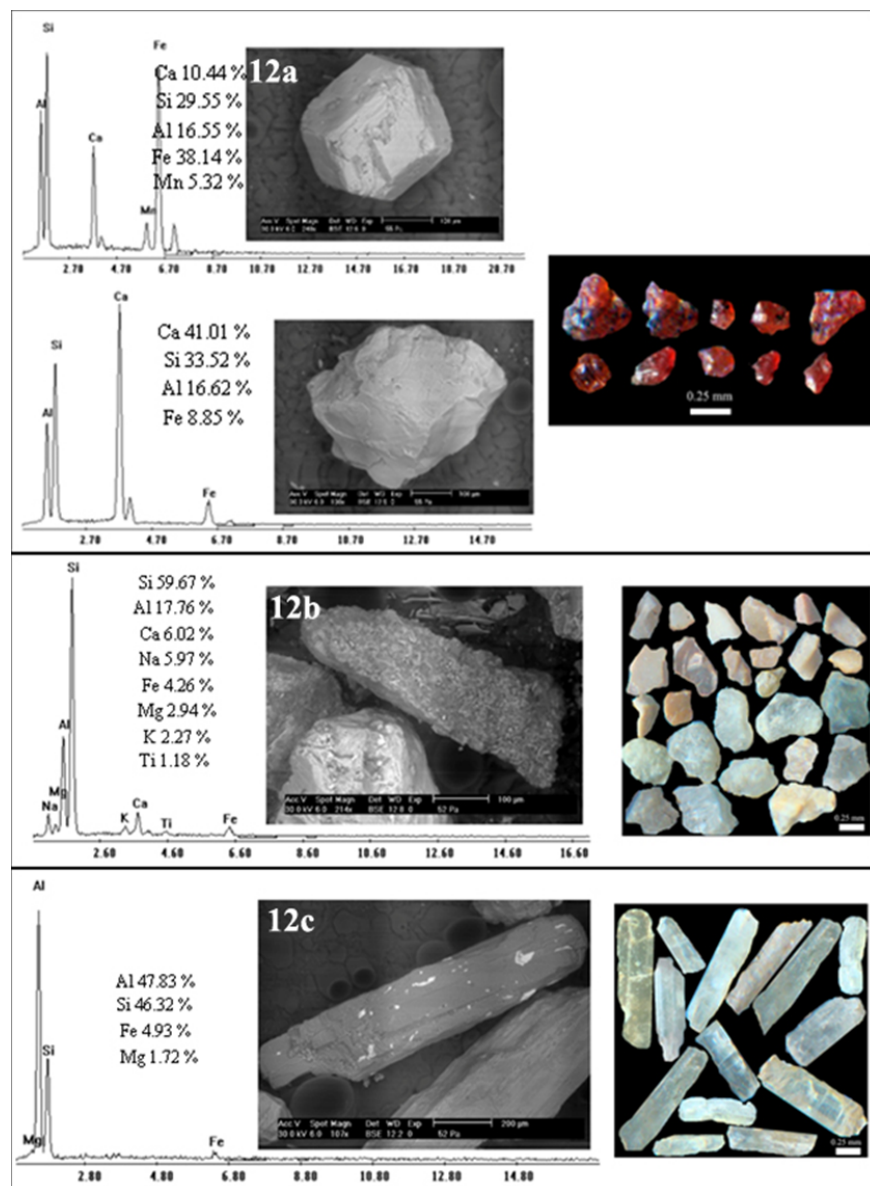
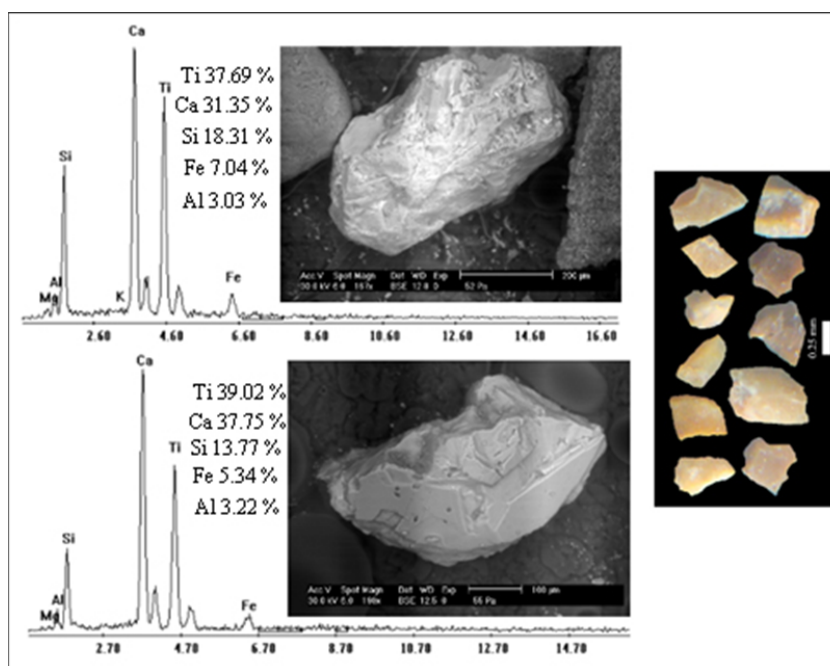


Fig. 13: EDX semi-quantitative chemical analysis (Wt %), BSE and photomicrograph of sphene mineral.



Fluorite varies from colorless to grey color with vitreous luster. Also, it ranges from transparent to translucent, a single crystal can be multi colored.

Citrine represented angular to slightly rounded yellow grains.

Source rocks of heavy minerals

The heavy minerals encountered in the stream sediment along the Sheikh Abdel Aal Tomb -El-Fawakhir mine point to several sources. The presence of pyroxene (clino-ortho-), hornblende, olivine, magnetite and titanomagnetite points essentially to basic igneous rocks (gabbroic rocks, dolomite and basaltic rocks). The basic igneous rocks are encountered in the Abu Ziran, Wadi El-Haramiya, Um Selimate, Wadi Attala regions.

The presence of gemstone yellow quartz (citrine) comes from quartz plugs of Wadi El-Haramiya. Fluorite and barite derived from Sodmain fluorite mine. Goethite after pyrite which derived from El- Sid gold mine.

Muscovite, biotite, albite plagioclase, potash feldspar, rutile, titanite (sphene), apatite and epidote points to acidic igneous rocks. The acidic igneous rocks in the studied district represented by alkali feldspar granites, granodiorites, tonalite, quartz diorite, monzogranite, syenogranites, rhyolite which exposed at Meatiq, Abu Ziran, El-Fawakhir and Wadi Attala. Tourmaline comes from pegmatites and pegmatitic granites. Olivine, magnetite, titanomagnetite and ilmenite derived from mafic-ultramafic rocks of El-Fawakhir ophiolite sequences. The presence of sillimanite, biotite, muscovite, titanite, epidote and garnet minerals point to metamorphic rocks exposed at Abu Fannani Formation in Meatiq area and Abu Ziran area.

CONCLUSIONS

From the grain-size analysis and heavy minerals separation of twenty-eight stream sediments in the area between El-Sheikh Abdelal – El-Fawakhir, Qift-El Quseir Road, Central Eastern Desert, the important conclusions drawn are as follows: The frequency curves reflect variable current velocities and turbulence of the transporting medium or it could suggest that the grains were from different sources.

The graphic mean value indicates the dominance of very coarse sand-size particles. The sediments, in general, show poorly sorting and are dominantly fine-skewed in nature. The poorly sorting is probably due to the coarser nature of the sediments. And may be due to the impact of intermixing and influx of the

sediments from different types of surrounding rock units. The studied sediments show wide range value of the kurtosis (very platykurtic to extremely leptokurtic) which suggests that the studied sediments achieved there sorting elsewhere in high-energy environment and indicates multiple environment i.e. one derived from riverine/aeolian environment.

The heavy minerals are thus classified into magnetic and non-magnetic minerals. The former comprises only the magnetite and goethite, however the latter minerals are classified into metallic and non-metallic minerals. The metallic mineral rutile. The non-metallic minerals are represented by albite, apatite, tourmaline, sphene, fluorite, cetrine, sillimanite and garnet, as well as mafic minerals represented by pyroxene, biotite, hornblende, olivine and epidote.

The concentration and distribution of the investigated heavy minerals suggest that the basic and acidic igneous rocks encountered in the Abu Ziran, Wadi El-Haramiya, Um Selimate, Wadi Attala regions and quartz plugs of Wadi El-Haramiya, Sodmain fluorite and El- Sid gold mines, pegmatites and metamorphic rocks exposed at Abu Fannani Formation in Meatiq area and Abu Ziran area are the main source of he detected light and heavy minerals.

REFERENCES

- Abdulkarim, R. Akintoye, A. E. Oguwuike, I. D. Imhansoeleva, T. M. Philips, I. M. Ruth, F. B. Olubukola, S. O. Rasheed, J. O. and Banji, A. O. (2011): Sedimentological variation in beach sediments of the barrier bar lagoon coastal system, South-western Nigeria. *Nature and Sci.*, 9, 19-26.
- Akaad, M. M. and Noweir, A. M. (1980): Geology and lithostratigraphy of the Arabian Desert orogenic belt of Egypt between lat. 25° 35' and 26° 30' N. I, *A. G. Bull.*, (Jeddah), 3, 4, 127-134.
- Attia, G. M., El Hadary, A. F., El Azab, A., El Gawad, A. and Ayatollah, E. A. (2015): Sedimentation and mineralization of Ria El-Gerrah, El-Gidami and El-Missikat Wadi sediments, Central Eastern Desert, Egypt. *J. Sediment. Soc. Egypt*, 22, 203-216.
- Amireh, B. S. (2014): Grain size analysis of the Lower Cambrian-Lower Cretaceous clastic sequence of Jordan, Sedimentological and paleo-hydrodynamical implications, *J. of Asian Earth Sci.*, 97, 67-88.
- Avramidis P. Samiotis A. Kalimani E. Papoulis D. Lampropoulou P. and Bekiari V. (2012): Sediment characteristics and water physicochemical parameters of the Lysimachia Lake, Western Greece. *Environ Earth Sci.*, 70 (1), 383-392.
- Baruah, J. Kotoky. P. and Sarma, J. N. (1997): Textural and Geochemical study on river sediments: A case study on the Jhanji River, Assam. *J. Indian Assoc. Sedimentologists*, 16, 195-206.
- Blott, S. J. and Pye, K. (2001): GRADISTAT: a grain size distribution and statistics package for the analysis of unconsolidated sediments. *Earth Surface Processes and Landforms*, 26, 237-1248.
- Carver, R. W. (1971): Procedures in sedimentary petrology. John Wiles, New York, 458p.
- Deer W. A. Howie R. A. and Zussman J. (2001): An introduction to the rock-forming minerals. 2nd Ed., Longman, London, 972p.
- El Ramly, M. F., (1972): A new geological map for the basement rocks in the Eastern and South-western Deserts of Egypt: *Ann. Geol. Sur. Egypt*, V, II, pp. 1-18.
- Folk, R. L. (1954): The distinction between grain size and mineral composition in sedimentary-rock nomenclature. *J. Geol.*, 62, 344– 359.
- Folk, R. L. and Ward, W. C. (1957): Brazos River Bar: A study in the significance of grain size parameters. *J. Sed. Pet.*, 27, 3-27.
- Geological Survey of Egypt (1992): Geological map of Egypt, Scale (1: 500,000), NG 36 K, sheet.
- Goldschmidt, V. M. (1954): Geochemistry: Clarendon Press, Oxford, 730 p.
- Hassaan, M. M., El-Desoky, H. M. and El-Kady, A. M. (2014): Homrit Waggat Feldspar Sands; Sedimentological Features, Mineralogical Composition and Suitability for Ceramics Industry, Central Eastern Desert, Egypt. *Inter. J. Innovative Sci., Engineering & Technology*, 1(10), 43-56.
- Kröner, A. Krüger, J. Rashwan, A. A. (1994): Age and tectonic setting of granitoid gneisses in the Eastern Desert of Egypt and south-west Sinai. *Geol. Rundsch.*, 83, 502–513.

Sedimentological and Heavy Minerals Studies On Stream Sediments

- Morsy, M. A. (2000): Application of multivariate statistics to study stream sediments data from the vicinity of lead-zinc occurrences at Gabal Rusas area, Eastern Desert, Egypt. *International Archives of Photogrammetry and Remote Sensing*, XXXIII, B7, 901-904.
- Muhs D. R. (2013): Loess and its geomorphic, stratigraphic, and paleoclimatic significance in the Quaternary. In: Shroder J (Editor in Chief), Lancaster N, Sherman DJ, Baas ACW (eds) *Treatise on Geomorphology*, v. 11. Academic Press, San Diego, Aeolian Geomorphology, 149–183.
- Rajaganapathi, V. C. Jitheshkumar, N. Sundararajan, M. Bhat, K. H. and Velusamy, S. (2013): Grain size analysis and characterization of sedimentary environment along Thiruchendar coast, Tamilnadu, India, *Arabian J. of Geosci.*, 6, 4717-4728.
- Rajasekhara Reddy, D. Karuna Karudu, T. and Deva Varma, D. (2008): Textural characteristics of south western part of Mahanadi Delta, east coast of India. *J. Ind. Assoc. Sed.*, 27, (1), 111-121.
- Singarasubramanian S. R. Mukesh M. V. Manoharan K. Murugan S. Bakkiaraj D. and John Peter A. (2006): Sediment characteristics of the M-9 tsunami event between Rameswaram and Thoothukudi, Gulf of Mannar, Southeast Coast of India. *Sci Tsunami Hazards*, 25, 160–172
- Venkatraman S. Ramkumar T. Anitha Mary I. and Ramesh G. R. (2010): Variations in texture of beach sediments in the vicinity of the Tirumalairajanar River mouth of India. *Int. J. Sed. Res.*, 26, 460–470.
- Venkatramanan, S. Ramkumar, T. Anithamari, I. and Ramesh, G. (2011): Variation in texture of beach sediments in the vicinity of the Thirumalairajanar river mouth of India, *Inter. J. Sed. Res.*, 26, 460-470.
- Watson, E. B. Pasternack, G. B. Gray, A. B. Goni, M. and Woolfolk, A. M. (2013): Particle size characterization of historic sediment deposition from a closed estuarine lagoon, Central California, *Estuarine. Coastal and Shelf Science*, 126, 23-33.

Elshahat, O. R.

دراسة الرسوبيات والمعادن الثقيلة على الرواسب الوديانية ، ضريح الشيخ عبدالعال-الفواخير، وسط الصحراء الشرقية،

مصر

اسامه رمزي الشحات

قسم الجيولوجيا - كلية العلوم - جامعة الأزهر

الخلاصة

اثبتت الدراسات النسيجية للرواسب النهرية بمنطقة الفواخير بوسط الصحراء الشرقية ان المكون الأساسى لهذه الرسوبيات هو حجم الحصى والرمل بينما حجم السلت قليل ومتغير فى العينات . يمكن تصنيف العينات المدروسة إلى نوعين يتميز النوع الأول منها بمحتوى كبير من الحصى ويشمل الحصى الرملى والحصى الرملى الطينى (١٩ عينة). بينما يتكون النوع الثانى من خليط من الحصى والرمل بنسب مختلفة، وتصنف على أنها رمل الحصى ورمل قليل الحصى (٩ عينات) . وتصنف الرواسب على انها رديئة الفرز، وعدم اتزان يتراوح من دقيقة جدا إلى كبيرة جدا ترسبت فى بيئات نهريّة تحت مستويات معتدلة إلى منخفضة من الطاقة .

من خلال الدراسات المعدنية، تتمثل المعادن الخفيفة فى الكوارتز، المسكوفيت و الفلسبار البوتاس (بنسب تصل إلى ٨٨.٥% - ٦.٩٢% - ٤.٥٢% على التوالى) ، بينما تنقسم المعادن الثقيلة إلى معادن المغناطيسية وغير مغناطيسية. وتشمل المعادن المغناطيسية على الماجنتيت والجوتايت، أما المعادن الغير مغناطيسية فتصنيف إلى معادن فلزية (متمثلة فى الروتيل) وغير فلزية تتكون من قبل ألبيت، أباتيت، سفين، سلمنيت ، سيترين، فلوريت ، التورمالين جارنت بالإضافة إلى المعادن قاتمة اللون (البيروكسين، البيوتيت، هورنبلند و إبيدوت) .

تشير المعادن الثقيلة التى تم التعرف عليها إلى عدة مصادر منها الصخور النارية القاعدية والحمضية والصخور المتحولة فى مناطق وادى عطا الله ، وادى الحراميه ، ابوزيران ، أم سليمان ، ابو فنانى وجبل معيتق .